ELSEVIER

Journal of Nuclear Materials 296 (2001) 192–202

journal of nuclear materials

www.elsevier.com/locate/jnucmat

Auger electron spectroscopy study of alloy 718 and 304L stainless steel irradiated with 800 MeV protons

M. García-Mazarío *, M. Hernández-Mayoral, A.M. Lancha

CIEMAT, Avenida Complutense 22, 28040 Madrid, Spain

Abstract

It is well known that radiation produces changes in materials microstructure such as formation of defects, dissolution and redistribution of secondary phases, precipitation of new phases, etc. and changes in the grain boundary microchemistry by a process known as radiation-induced segregation (RIS). This paper describes the grain boundary microchemical characterization of alloy 718 and 304L stainless steel irradiated with high-energy protons at Los Alamos Neutron Science Center (LANSCE), performed by means of Auger electron spectroscopy (AES). In addition, non-irradiated alloy 718 was characterized as reference. The Auger results showed that as a consequence of exposure to proton radiation, the changes observed in alloy 718 were the disappearance of the nickel and niobium rich grain boundaries precipitates and RIS of the major alloying elements (nickel to grain boundaries, and chromium and iron away from grain boundaries). On the other hand, in irradiated AISI 304L no differences were observed between intergranular and transgranular areas.

1. Introduction

In spallation sources, the neutrons are generated by protons of around 1 GeV energy, which cause spallation of the nuclei in a heavy metal target. Radiation damage by the high-energy protons and neutrons is crucial for the lifetime of structural materials in or close to the proton beam. The Water Degrader (WD) of the spallation source of Los Alamos Neutron Science Center (LANSCE) consists of two concentric spherical shells made of alloy 718 and AISI 304L and it is considered the component with the highest irradiation load in a spallation environment available up to now [1,2].

Alloy 718 is a nickel base alloy that presents a high strength and corrosion resistance. It has an austenitic matrix hardened by precipitation of the fcc $\gamma'[Ni_3(Al, Nb, Ti)]$ and the bct $\gamma''[Ni_3(Al, Nb, Ti)]$ phases. In addition, other phases such as $\delta(Ni_3Nb)$, Laves (Ni_2Nb), and MC-type carbides have been observed in this material. On the other hand, AISI 304L is an austenitic stainless steel with low carbon content.

It is known that radiation produces changes in materials microstructure such as formation of defects, dissolution and redistribution of secondary phases, precipitation of new phases, etc. Among the changes reported for the alloy 718 are the loss of the γ'' particles through the matrix and at the grain boundaries, the redistribution of the γ' with refined particle sizes [3], and furthermore, the disappearance of most of the carbide precipitates at grain boundaries [1]. Microstructural changes for 304L involve an increase of the density of defects and no precipitation or phase instabilities are usually observed [4], although in some studies, austenite (γ) to ferrite (α) phase transformation has been reported [5].

In addition to microstructural changes, radiation produces changes in the grain boundary microchemistry by a process known as radiation-induced segregation (RIS). Two mechanisms have been proposed for RIS [6]. One is the preferential exchange of an alloying element with the vacancy flux resulting in a net solute flux towards or away from the boundary. Slow diffusing elements such as nickel enrich and fast diffusing elements such as chromium and iron deplete the grain boundaries.

* Corresponding author. Tel.: +34-91 346 6618; fax: +34-91 346 6661.

E-mail address: m.mazario@ciemat.es (M. García-Mazarío).

0022-3115/01/$ - see front matter
PII: S0022-3115(01)00518-9

The second mechanism is the preferential association of undersized atoms with the interstitial flux. Solutes that are significantly undersized enrich at grain boundaries. In the case of ternary Fe–Cr–Ni alloys it has been shown that the vacancy exchange mechanism explains the observed major alloying element segregation. Other solutes with significant size misfits do segregate by the interstitial association mechanism.

Therefore, the radiation-induced material changes are expected to affect the performance of these materials, alloy 718 and AISI 304L. The radiation-induced changes and damage in fission and fusion materials have been widely reported, but the information in the case of materials of spallation sources is very limited.

The present paper describes the grain boundary microchemical characterization performed by means of Auger electron spectroscopy (AES) of alloy 718 and AISI 304L irradiated with high-energy protons, 800 MeV, at LANSCE. In addition, non-irradiated alloy 718 has been characterized as reference. This study has been carried out with the aim to determine the changes that radiation produces in the grain boundary microchemistry and to relate them with the previously studied mechanical behavior of these materials [1,2].

2. Experimental

2.1. Material

The materials studied were the irradiated and non-irradiated nickel base alloy 718 and the irradiated stainless steel AISI 304L. Both irradiated materials come from the LANSCE water degrader and have been irradiated with 800 MeV protons to a total dose of 5.3 Ah. The maximum fluence calculated is 2.9×10^{25} p/m^2 corresponding to a displacement dose of about 8.5 dpa. The flux of neutrons was very low and their contribution was estimated to be a few percent of the proton value. The maximum temperature during the irradiation never exceeded 250°C [1,2].

One sample of irradiated alloy 718 and one sample of irradiated AISI 304L were analyzed at CIEMAT. In addition, two samples of non-irradiated alloy 718 were studied as reference material. Non-irradiated samples of AISI 304L were not analyzed. The dimensions of the samples of irradiated and non-irradiated alloy 718 were 1 mm × 0.5 mm × 10 mm. The sample of AISI 304L was a bit larger, with dimensions of 1.6 mm × 0.5 mm × 10 mm.

According to the information supplied [1], the chemical composition of the irradiated alloy 718 sample is shown in Table 1. The heat treatment applied to the alloy was: annealing at 1065°C for 1 h and air cooling, afterwards, aging at 760°C for 10 h, then furnace cooling to 650°C at 55°C/h and holding at 650°C for a total time of 20 h. As a reference (non-irradiated) material, an alloy 718 from a different source had to be used since no original material was available. However it is believed, [1], that the compositions and heat treatments were almost identical for both materials.

Regarding AISI 304L, it was solution annealed and its chemical composition is shown in Table 2 [2].

2.2. Auger electron spectroscopy

The instrument used was a PHI 660 Scanning Auger Microprobe, which has a spatial resolution of approximately 100 nm allowing analysis in small spots. In order to promote the intergranular fracture necessary to perform interface segregation studies by this technique, samples from non-irradiated and irradiated alloy 718 and from irradiated AISI 304L were cathodically charged with hydrogen in a solution 0.1 N of H_2SO_4 with the addition of As_2O_3 as a poison for the recombination of hydrogen. The solution temperature was 70°C and the period of charge was 48 h. Afterwards, samples were fractured by tension at a deformation rate of 1 μm/s inside the Auger vacuum chamber, at a pressure of 10^9 Torr, with a specially designed fracture stage attached to the spectrometer that allows to analyze the two surfaces obtained after the fracture. Once the

Table 1
Chemical composition of alloy 718 (wt%)

Ni	Cr	Fe	Nb	Mo	Ti	Others
53	18	18	5	3	1	2

Table 2
Chemical composition of 304L stainless steel (wt%)

C	Si	Mn	P	S	Cu	Cr	**Ni**	Mo	N	Others	Fe
0.012	0.46	1.75	0.027	0.023	0.22	18.95	10.37	0.24	0.058	0.191	Bal.

fracture was achieved, a secondary electron image of the fracture surface was obtained to identify the areas of the sample that failed intergranularly. Spot analyses were performed on grain boundary facets and on ductile fracture for comparison.

Spectra were collected using a beam energy of 10 keV and a target current of 0.3 μA. The atomic concentrations were calculated according to Ref. [7]. Composition depth profiles were performed using a 2 keV argon ion flux rastered over a 2 mm × 2 mm area and with a pressure of argon of 5 mPa, yielding a sputter rate of about 2 nm/min calibrated with a Ta_2O_5 foil of known thickness.

3. Results

3.1. Non-irradiated alloy 718

3.1.1. Microstructure and microhardness

The microstructure of non-irradiated alloy 718 reference material supplied was examined by scanning electron microscopy (SEM) and it is presented in Fig. 1. As it can be seen, needle-like shaped precipitates, small particles and coarse precipitate phases appear along the austenitic grain boundaries and also throughout the grains. Microhardness measurements, performed with a load of 2 N (HV 0.2) showed a value of 450 ± 16 HV. This result is the average of 10 identations.

3.1.2. Microchemistry

Two samples of non-irradiated alloy 718 were fractured, both samples showed intergranular facets. Fig. 2(a) shows, as an example, an SEM image of one of the fracture surfaces obtained. Two zones may be differentiated, a zone in the middle of the fracture surface with ductile appearance and a zone around the ductile zone, along the edge of the fracture surface in which some facets with intergranular appearance may be distinguished. Fig. 2(b) also shows a detail of one zone of this fracture surface showing some intergranular facets and the areas where the Auger analyses were performed.

A total of 70 analyses were performed on this material, 57 of which were taken from intergranular areas and 13 from ductile areas. As an example, Fig. 3 shows three Auger spectra obtained from the fracture surface of the non-irradiated alloy 718. Fig. 3(a) corresponds to a ductile area and Figs. 3(b) and (c) were taken from intergranular areas. In spectra Figs. 3(a) and (b), in ductile as well as in intergranular areas, the presence of the main elements of the alloy (nickel, chromium and iron) and the minor elements (niobium, titanium and molybdenum) can be observed, together with carbon and oxygen from contamination. In some of the intergranular areas no molybdenum was detected, Fig. 3(c). Comparing the spectra of the ductile and intergranular areas, higher peaks of niobium and lower peaks of

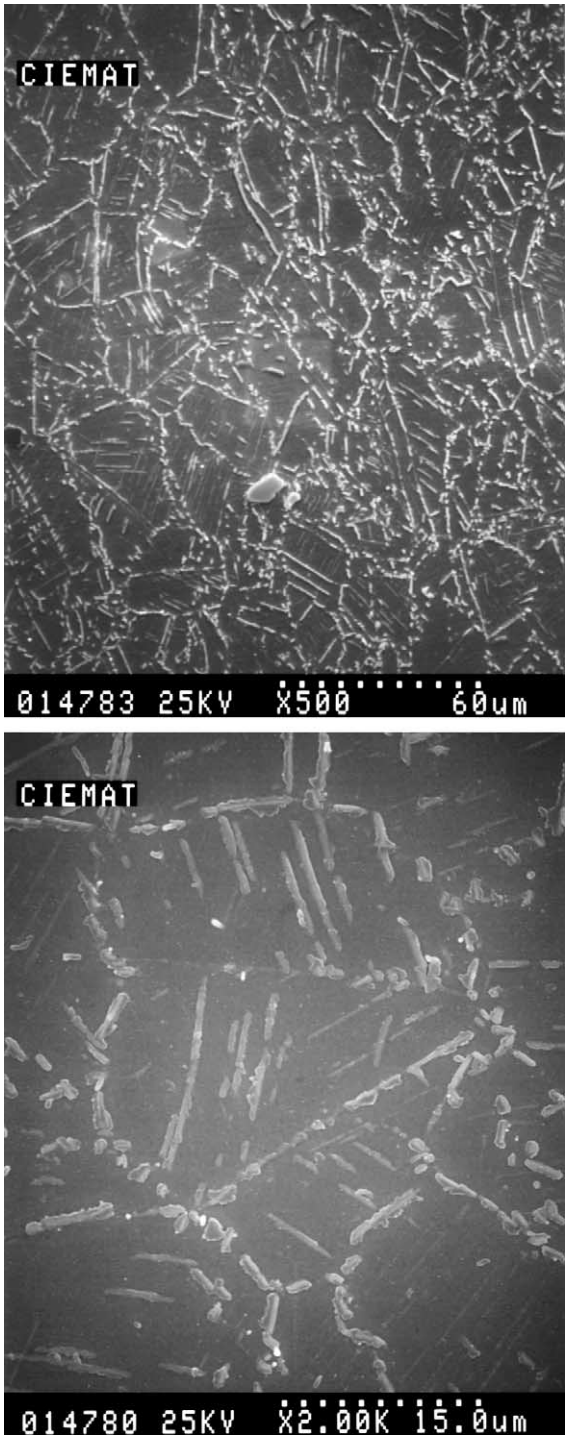

Fig. 1. SEM images of microstructure of non-irradiated alloy 718.

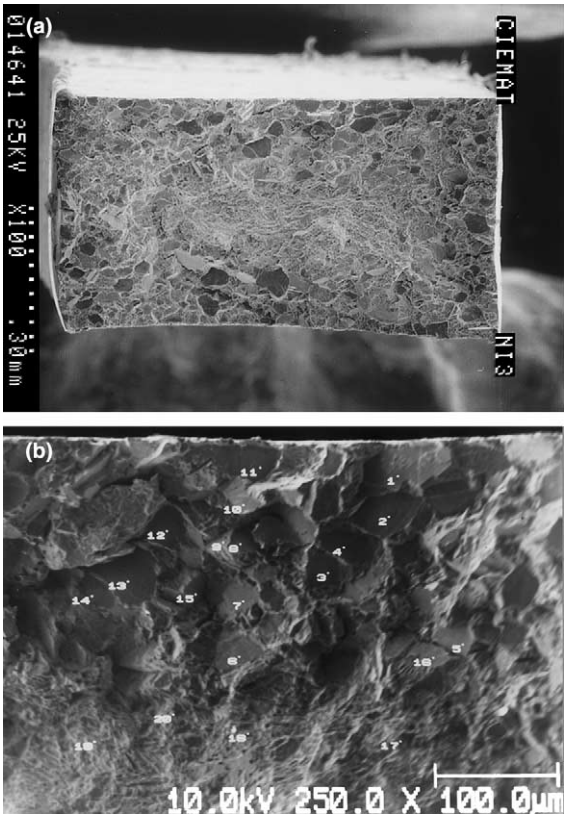

Fig. 2. Non-irradiated alloy 718: (a) image of fracture surface; (b) detail of fracture surface.

chromium and iron were observed at the intergranular areas than at the ductile areas.

Quantitative results are represented in the form of histograms, Fig. 4, where the atomic concentration of the alloying elements versus the position, intergranular or ductile, is shown. The average concentrations and standard deviation of these elements were calculated in the ductile and intergranular zones. Horizontal discontinuous lines in the histograms indicate the average concentrations. In addition, these values are summarized in Table 3. Carbon and oxygen are not included in the quantification.

As it is shown in the table and in the figures, nickel average concentration at the intergranular zone is higher than at the ductile zone while iron and chromium show the opposite trend. With respect to the minor elements of the alloy, niobium has higher levels at the intergranular zone than at the ductile zone. In the case of molybdenum, the average concentration at ductile and intergranular zone is similar, although a 25% of the intergranular areas analyzed does not show molybdenum as can be observed in the histogram. Finally, titanium average concentration is slightly higher at the intergranular zone than at the ductile zone.

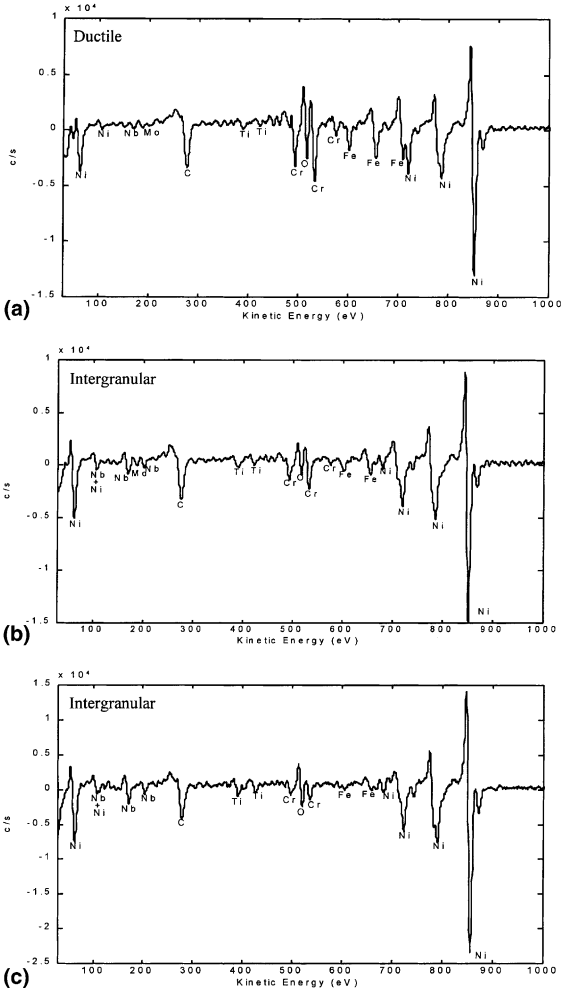

Fig. 3. Auger spectra on fracture surface of non-irradiated alloy 718. (a) Ductile area. (b) and (c) Intergranular areas.

Depth composition profiles were performed in four intergranular areas and in one ductile area for comparison. Fig. 5 shows two depth profiles where the atomic concentration versus depth is represented from a ductile and from an intergranular area. The depth profile of the ductile area is flat and no changes in the composition of the elements are observed. In the four intergranular areas, nickel and niobium enrichment together with chromium and iron depletion were observed. As can be seen in Fig. 5(b), a relation between nickel and niobium seems to exist because their concentrations change in the same way. The thickness of the layer showing nickel and niobium enrichment and chromium and iron depletion was approximately 25 nm in two of the four areas and more than 40 nm in the other two. With respect to molybdenum and titanium, they stayed constant during all the depth.

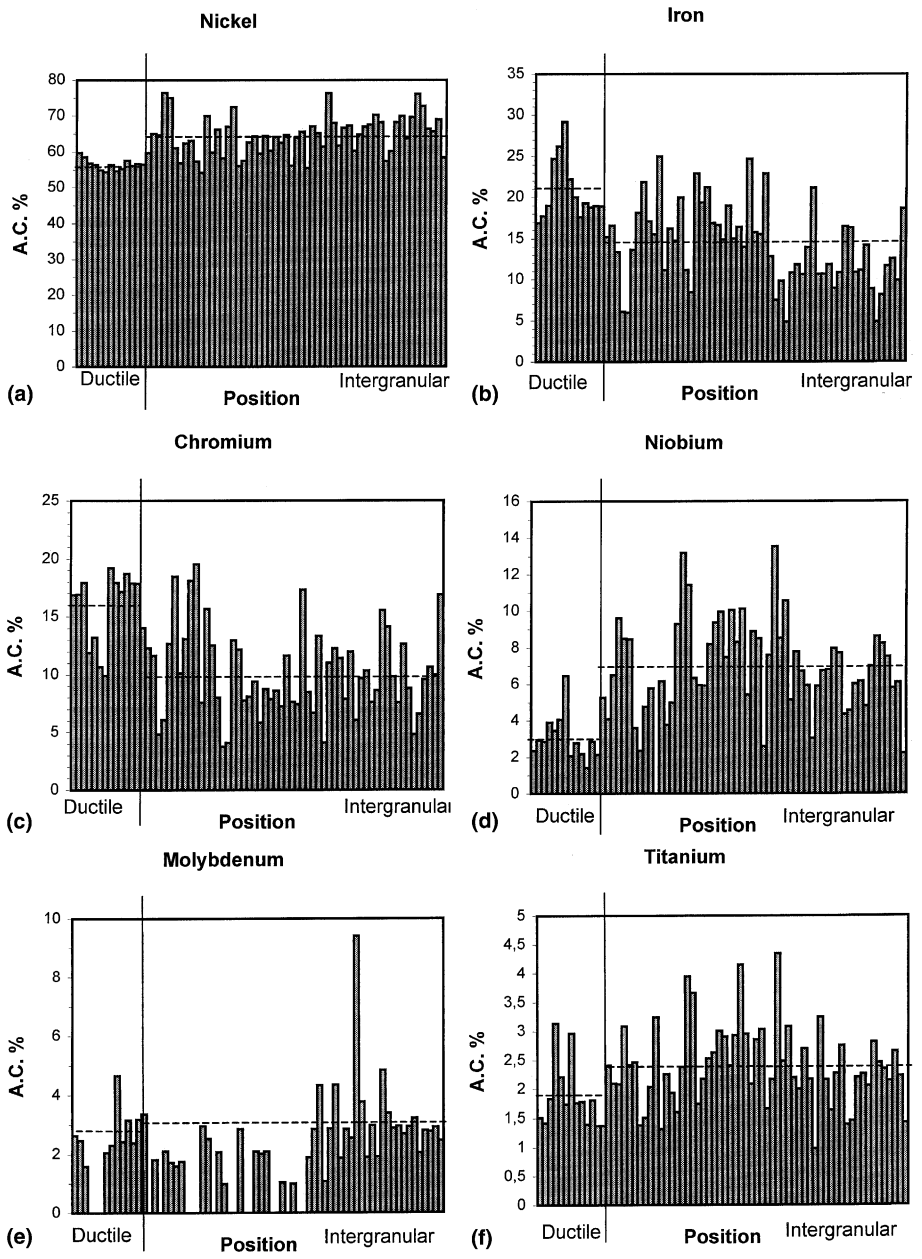

Fig. 4. Histograms showing different element concentrations on fracture surface of non-irradiated alloy 718: (a) nickel; (b) iron; (c) chromium; (d) niobium; (e) molybdenum; (f) titanium.

Table 3
Average concentration of the alloying elements at ductile and intergranular areas in non-irradiated alloy 718 (at.%)

	Ni	Fe	Cr	Nb	Mo	Ti
Ductile	56 ± 2	21 ± 4	16 ± 3	3 ± 1	2.7 ± 0.8	1.9 ± 0.6
Intergranular	64 ± 5	14 ± 5	10 ± 4	7 ± 3	3 ± 1	2.4 ± 0.7

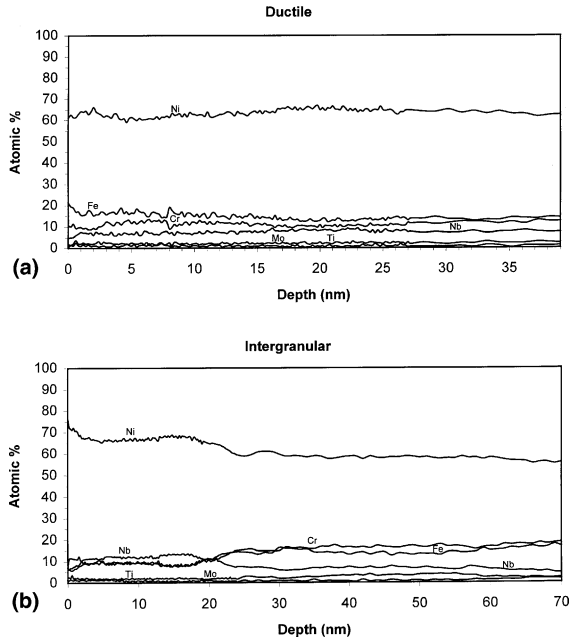

Fig. 5. Depth profile performed on fracture surface of non-irradiated alloy 718: (a) ductile area; (b) intergranular area.

3.2. Irradiated alloy 718

Fig. 6(a) shows an image of the fracture surface obtained in alloy 718 irradiated where it can be observed that almost all the fracture surface shows an intergranular appearance while no clear ductile zone can be distinguished. For this reason, ductile areas of the non-irradiated alloy 718 were used as reference. Fig. 6(b) shows a detail of the fracture surface where the areas in which the intergranular Auger analyses were performed are indicated.

A total of 27 intergranular analyses were taken from the fracture surface of alloy 718 irradiated, an example is shown in Fig. 7, where the presence of the main alloying elements nickel, chromium and iron, the minor alloying elements, niobium and titanium and also carbon and oxygen from contamination were observed. Molybdenum was observed only in 22% of the intergranular areas analyzed. Qualitatively, comparing the spectrum of the intergranular areas, Fig. 7, to the spectrum of reference ductile areas, Fig. 3(a), higher peaks of iron and chromium were seen at the reference ductile spectrum than at the intergranular areas.

Regarding quantitative results, Fig. 8 shows the histograms of nickel, chromium, iron, niobium, molybdenum and titanium and Table 4 shows the average concentration and the standard deviation of these elements.

Nickel shows higher levels at intergranular areas than at reference ductile areas, this enrichment being higher

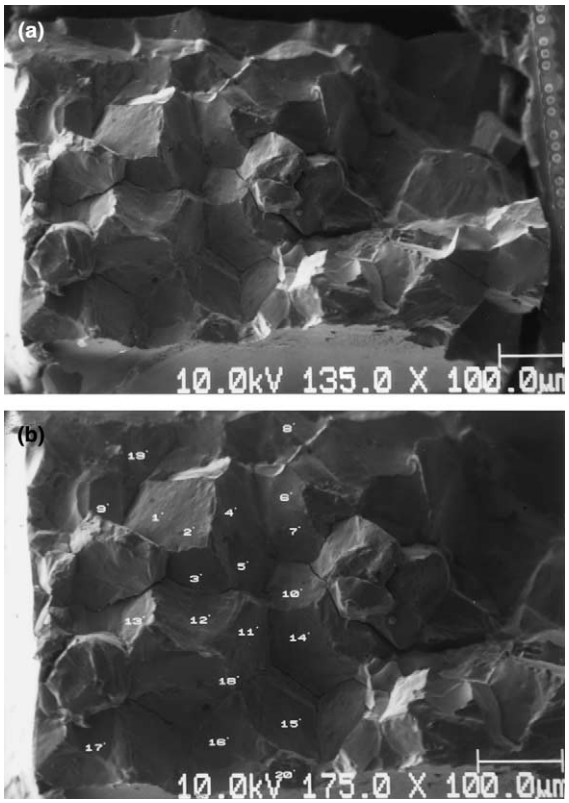

Fig. 6. Irradiated alloy 718: (a) image of fracture surface; (b) detail of fracture surface.

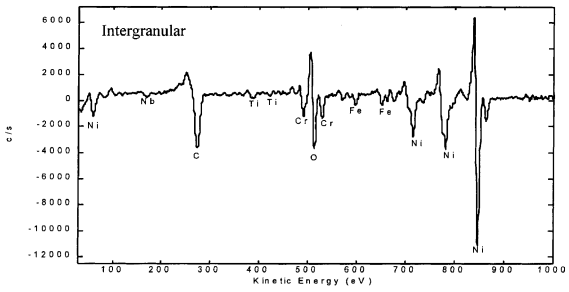

Fig. 7. Auger spectrum on fracture surface of irradiated alloy 718. Intergranular area.

than that observed at the intergranular areas in the non-irradiated material. Iron levels were lower at the intergranular zone than at the reference ductile zone. With respect to chromium lower levels of this element were seen at the intergranular zone than at the reference ductile zone. The levels of iron and chromium were lower than those observed for the non-irradiated alloy 718.

Regarding niobium, average concentrations are equal at the intergranular and at the reference ductile zones. It

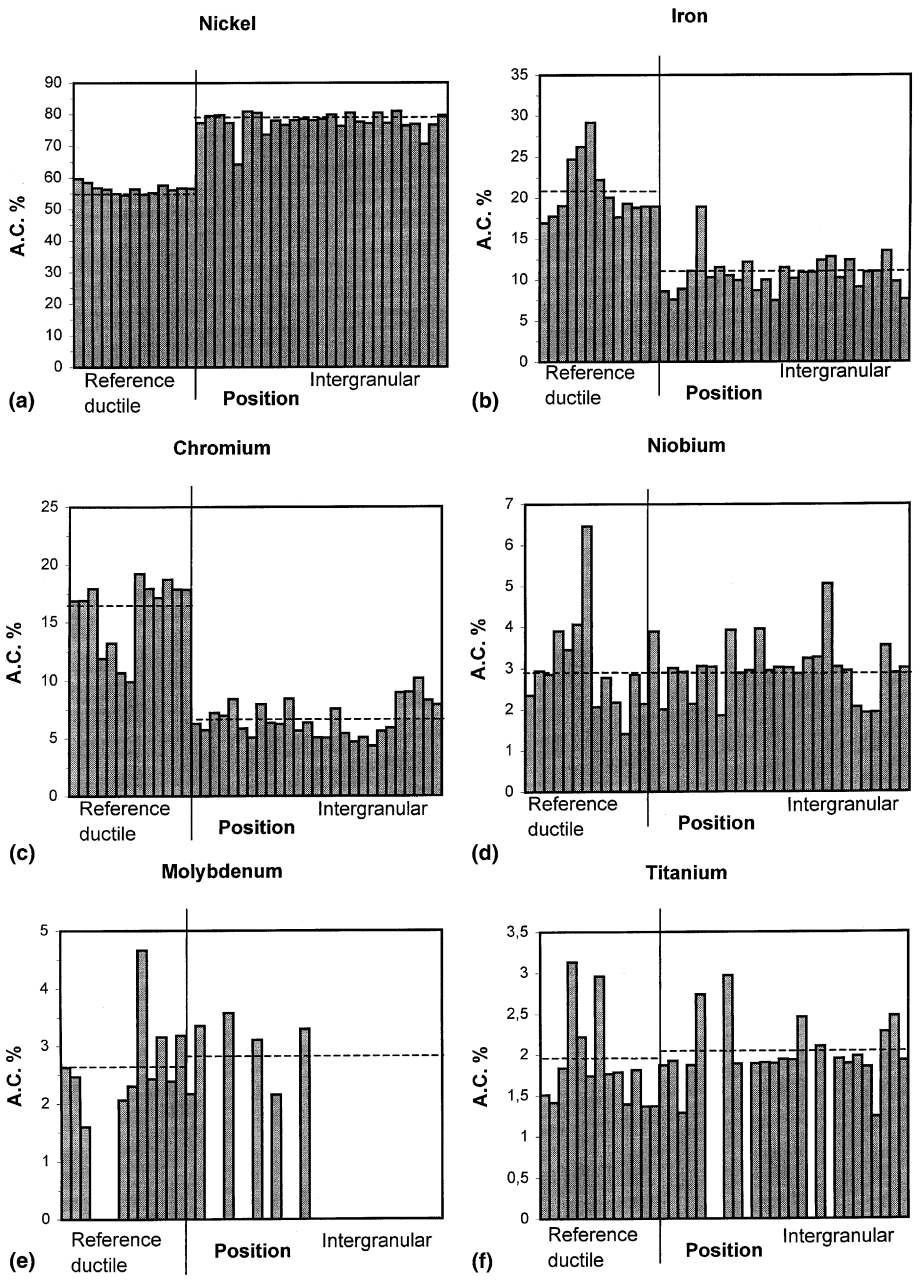

Fig. 8. Histograms showing different element concentrations on fracture surfaces of irradiated alloy 718: (a) nickel; (b) iron; (c) chromium; (d) niobium; (e) molybdenum; (f) titanium.

Table 4
Average concentration of the alloying elements at reference ductile and intergranular areas in irradiated alloy 718 (at.%)

	Ni	Fe	Cr	Nb	Mo	Ti
Reference ductile (non-irradiated alloy 718)	56 ± 2	214	16 ± 3	3 ± 1	2.7 ± 0.8	1.9 ± 0.6
Intergranular	77 ± 3	11 ± 2	7 ± 2	3 ± 0.7	2.9 ± 0.6	2.0 ± 0.4

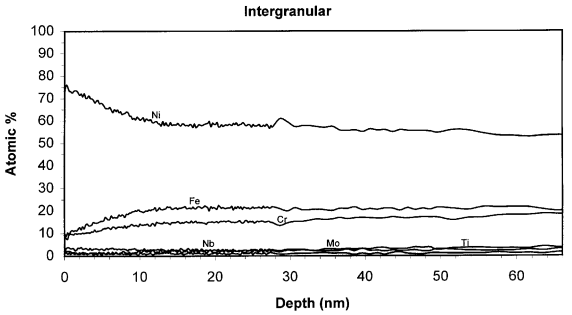

Fig. 9. Depth profile performed on fracture surface of irradiated alloy 718. Intergranular area.

is worth mentioning that higher levels of niobium were observed in the intergranular zone than in the ductile zone in the case of non-irradiated alloy 718. Molybdenum appears in the intergranular areas with an average concentration similar to the reference ductile areas. Finally, titanium was detected in almost all the intergranular zones with an average concentration also similar to the reference ductile zone.

Depth composition profiles were performed in four intergranular areas. Fig. 9 shows one of the depth profiles obtained. Three of the areas analyzed showed nickel enrichment and chromium and iron depletion up to a maximum depth of 10 nm, as can be seen in this figure. Niobium, molybdenum and titanium concentrations were constants during all the profile. The other area showed a layer of about 5 nm with a high concentration of niobium accompanied by a high concentration of carbon suggesting the presence of niobium carbide.

3.3. Irradiated AISI 304L

As the dimension of the sample received was wider than the size of the sample holder hole, special sample holders had to be manufactured. In spite of being cleaned repeatedly with water, acetone and alcohol in ultrasonics, under the ultrahigh vacuum of the AES chamber, the new sample holders outgassed chlorine from the refrigerant used in their manufacture, which was subsequently deposited on the fresh fracture surfaces.

Intergranular fracture was obtained in the AISI 304L sample as can be seen in Fig. 10(a). In the photograph the presence of large grains at the right and left sides of the fracture surface, as well as transgranular fracture by quasi-cleavage at the center of the fracture surface, can be observed. No clear ductile zone was detected. Fig. 10(b) shows a detail of the fracture surface showing the intergranular areas and the positions where Auger analyses were performed.

As no clear ductile zone was observed, analyses on transgranular areas were taken as reference. From a

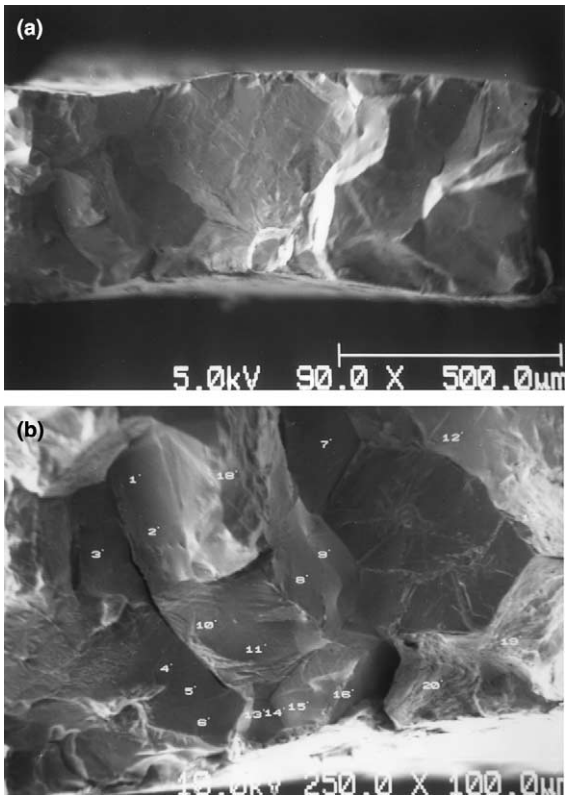

Fig. 10. Irradiated AISI 304L: (a) image of fracture surface; (b) detail of fracture surface.

total of 56 analyses, 46 were performed at intergranular areas and 10 at transgranular areas. Fig. 11 shows a typical Auger spectrum, where the presence of the main elements of the alloy, iron, chromium and nickel can be seen together with carbon, oxygen and chlorine from contamination. No qualitative differences were observed between transgranular and intergranular areas.

With respect to quantitative results, Table 5 shows the average concentration and the standard deviation of these elements at transgranular and intergranular areas.

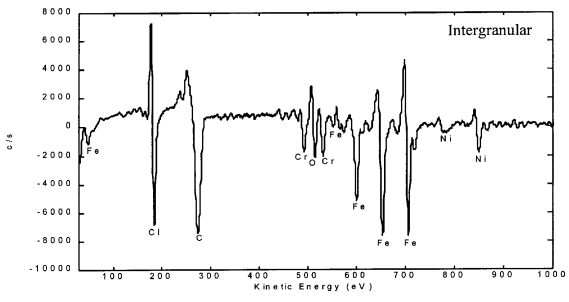

Fig. 11. Auger spectrum on fracture surface of irradiated AISI 304L. Intergranular area.

Table 5
Average concentration of Fe, Cr and Ni at transgranular and intergranular areas in irradiated AISI 304L (at.%)

	Fe	Cr	Ni
Transgranular	70 ± 2	18 ± 2	12 ± 1
Intergranular	72 ± 4	16 ± 4	12 ± 1

At the intergranular zone, the average concentration for iron is slightly higher and the average concentration of chromium is slightly lower than in the transgranular zone, but considering the deviations, these differences are not significant.

Depth profiles were also performed with the aim to know if segregation appeared below the layer of contamination, but no changes in the concentrations of iron, chromium and nickel were observed with depth, and no additional elements were observed after removing the layer of chlorine, carbon and oxygen.

4. Discussion

4.1. Alloy 718

Grain boundary microchemistry observed for non-irradiated alloy 718 consisted of a high concentration of nickel and niobium accompanied by a decrease of iron and chromium. This microchemistry can be associated to the presence of nickel and niobium rich particles at grain boundaries or can be attributed to segregation during heat treatments of nickel and niobium towards grain boundaries and migration of chromium and iron away from grain boundaries.

Looking at the possibility to attribute this microchemistry to precipitates, three kinds of phases have been reported to be found precipitated at grain boundaries in this material: the δ phase, the precipitation of which is caused by the first aging step at 760°C [8,9], the γ'' phase that can be formed at grain boundaries during aging [10], and niobium carbides, NbC(N), that can also be formed during aging [9,11].

Taking into account that the microstructure of this material presented precipitates along the grain boundaries, this nickel and niobium enrichment could probably be associated with the presence of these precipitates. The size of the precipitates observed in the microstructure seems to indicate that they are δ particles. In addition, two of the depth profiles performed at grain boundaries in this material showed thickness of nickel and niobium enrichment of more than 40 nm. This thickness could correspond to δ precipitates.

However, there are also studies in the literature [3,10,12] in which niobium enrichment was observed at the grain boundaries and was associated with the formation of γ'' precipitates at the grain boundaries. The size of γ'' precipitates is $\sim$ 5–30 nm [9]. Two of the depth profiles showed thickness of nickel and niobium enrichment of 25 nm that are in accordance with the size of γ'' precipitates.

As regards the possible presence of niobium carbides, it would justify the niobium enrichment but not the nickel enrichment. As the depth profiles performed showed that carbon disappeared after removing the first layers, indicating that it was carbon from contamination, it can be concluded that no carbides were present. However, it has to be considered that depth profiles have been performed only on four intergranular areas. The rest of the intergranular analyses were performed on the surface, without sputtering, and in them it is not possible to appreciate if all the carbon observed is from contamination or if there is also carbon in the form of carbides.

Then, the nickel and niobium enrichment could be the result of the precipitates observed in the microstructure of the material (possibly δ and γ'' precipitates), although the presence of niobium carbides precipitates at grain boundaries cannot be discarded.

Regarding the possibility to attribute the observed microchemistry at grain boundaries in alloy 718 to segregation of nickel and niobium to grain boundaries and chromium and iron diffusion away from grain boundaries, the thickness observed in the depth profiles, 25 or 40 nm, seems also to be reasonable for segregation. Segregation of niobium has been reported in several papers. According to some authors [10,12] niobium possibly segregates to the grain boundaries and promotes γ'' precipitation there during aging. Other studies [3] indicate that niobium can consistently enrich with nickel, but the excess of niobium might also be segregated to interfaces. No references in the literature have been found about nickel segregation to grain boundaries and chromium and iron diffusion away from grain boundaries in non-irradiated alloy 718.

In the current study, niobium enrichment seems to be associated with nickel enrichment suggesting that the microchemistry observed at grain boundaries is the result of the presence of nickel and niobium rich precipitates. However, it is not possible to know if all the niobium is in the form of precipitates or if there is also niobium segregated. Segregation to grain boundaries of other element has not been observed in the present study although segregation of phosphorus, sulfur and boron has been reported in this material submitted to different heat treatments [3,12,13].

After irradiation, the first change observed in alloy 718 is the appearance of the fracture surface which is almost completely intergranular, while in the non-irradiated material only disperse intergranular facets were observed. The grain boundary microchemistry obtained after irradiation indicates a high concentration of nickel accompanied by a decrease of iron and chromium. Re-

Table 6
Average concentration differences between intergranular and ductile zone

	Δ (intergranular–ductile)					
	Ni	Fe	Cr	Nb	Mo	Ti
Non-irradiated alloy 718	8	−7	−6	4	0.3	0.5
Irradiated alloy 718	21	−10	−9	0	0.2	0.1

garding niobium, molybdenum and titanium, no differences were observed in these elements between ductile and intergranular areas.

With the aim to compare with the non-irradiated material, Table 6 shows a parameter named Δ (intergranular–ductile), defined as the difference between the average concentration of the intergranular area and the average concentration in the ductile area, for the non-irradiated and irradiated material, respectively. Positive values indicate enrichment at grain boundaries while negative values show depletion at grain boundaries.

Nickel enrichment can be observed in both the non-irradiated and the irradiated material, but this enrichment is much higher in the case of the irradiated material. Iron and chromium depletion is observed at grain boundaries in both materials, the depletion is also higher in irradiated material, although it is less pronounced than the nickel enrichment. Niobium shows enrichment only in the non-irradiated condition. Finally molybdenum and titanium show a slight enrichment in both the non-irradiated and the irradiated material, but as it can be seen from their values in the results, the differences were not significant.

As regards molybdenum, it is worth mentioning Ref. [3] in which alloy 718 showed a high concentration of molybdenum at grain boundaries before being irradiated and a decrease of molybdenum at grain boundaries to the level of the matrix as a consequence of neutron irradiation. In the present study, no differences have been observed in molybdenum before and after irradiation.

Nickel enrichment and chromium and iron depletion are observed in the non-irradiated as well as in the irradiated alloy 718. However, niobium enrichment was not observed in the irradiated material, indicating clearly that in this case the nickel enrichment cannot be associated to precipitates, neither γ'' nor δ. According to Ref. [3] irradiation affects the stability of several phases. Changes attributed to radiation included the disappearance of γ'' at grain boundaries, while the other coarse precipitate phases in alloy 718, MC carbides and δ phase were not significantly changed in the irradiated material. However, the disappearance of most of the intergranular carbide precipitates was observed in this alloy 718 irradiated with 800 MeV protons [1].

In the current study, the microchemistry after irradiation indicates that the precipitates that were present in the non-irradiated material have disappeared. In addition, the layer showing nickel enrichment is too thin (10 nm, as it was shown in the depth profiles) to justify the presence of precipitates. Therefore, the nickel enrichment accompanied by the depletion of iron and chromium can be attributed to radiation-induced segregation. This thickness is in accordance with RIS profiles that are often characterized by their narrowness. RIS has indeed already been reported [3] in alloy 718.

4.2. AISI 304L

The microchemistry observed in irradiated AISI 304L at grain boundaries was similar to the composition observed at transgranular areas.

According to the literature a non-equilibrium segregation of chromium (presegregation of chromium) can occur during cooling from high temperatures in fabrication processes of AISI 304L [4,14–16]. If a presegregation of chromium would have existed in the material before irradiation, it could be thought that the radiation produced the diffusion of this element away from grain boundaries in accordance with the RIS theory. This fact would justify the microchemistry observed. It has been reported [4,15,16] that when presegregation exists, and afterwards the material is irradiated a typical W-shaped profile is observed at low doses, but after irradiation at higher doses the *W*-shaped chromium profile disappear and chromium depletion appears. In our case, the depth profiles obtained in this material show neither *W*-shape nor depletion of chromium. However, two factors have to be considered: non-irradiated AISI 304L was not studied and a ductile zone was not obtained at the fracture surface of the irradiated AISI 304L, therefore transgranular zone has been used as reference to compare with the microchemistry at grain boundaries. It would have been necessary to study AISI 304L before irradiation.

On the other hand, contamination of chlorine, carbon and oxygen could have masked the results, although depth profiles have been performed and no segregation has been observed after removing the contamination layer.

5. Conclusions

AES studies of alloy 718 and AISI 304L irradiated with 800 MeV protons have been performed with the aim to know the influence of irradiation on the microchemistry of grain boundaries in both materials. In order to compare the behavior under irradiation, alloy 718 without irradiation was also studied. No AISI 304L in the non-irradiated state has been studied.

- Grain boundary microchemistry observed in non-irradiated alloy 718 consisted of an enrichment of nickel and niobium accompanied by a depletion of iron and chromium. This microchemistry has been attributed to the presence of nickel and niobium rich particles at grain boundaries, possibly δ and γ'' precipitates, although the presence of niobium carbides precipitates at grain boundaries and/or niobium segregation to grain boundaries cannot be discarded.
- Grain boundary microchemistry observed in alloy 718 after proton irradiation to 8 dpa consisted of a high enrichment of nickel accompanied by a depletion of iron and chromium. The nickel enrichment and iron and chromium depletion were higher than in the non-irradiated material. No differences were observed in the concentration of niobium between ductile and intergranular areas. This microchemistry has been attributed to segregation of nickel towards grain boundaries and iron and chromium away from grain boundaries.
- As a consequence of exposure to proton radiation, the changes observed in alloy 718 have been the disappearance of the nickel and niobium rich grain boundaries precipitates and RIS of the major alloying elements (nickel to grain boundaries, and chromium and iron away from grain boundaries).
- In irradiated AISI 304L, no differences were observed between the intergranular and transgranular areas. This microchemistry could be a consequence of a possible presegregation of chromium in the material before irradiation, and diffusion of this element away from grain boundaries by irradiation. In order to confirm this, it would have been necessary the study of AISI 304L before irradiation. On the other hand, contamination of chlorine, carbon and oxygen could have masked the results.

References

[1] F. Carsughi, H. Derz, P. Ferguson, G. Pott, W. Sommer, H. Ullmaier, J. Nucl. Mater. 264 (1999) 78.
[2] J. Chen, Y. Dai, F. Carsughi, W.F. Sommer, G.S. Bauer, H. Ullmaier, J. Nucl. Mater. 275 (1999) 115.
[3] L.E. Thomas, S.M. Bruemmer, in: Proceedings of the Eighth International Symposium on Environmental Degradation of Materials in Nuclear Power Systems Water Reactors, Ed. American Nuclear Society, Amelia Island, FL, August 1997.
[4] S.M. Bruemer, E.P. Simonen, P.M. Scott, P.L. Andresen, G.S. Was, J. Nucl. Mater. 274 (1999) 299.
[5] W.J. Liu, C.H. Tsai, J.J. Kai, Scripta Metall. Mater. 30 (1994) 547.
[6] T.R. Allen, J.T. Busby, G.S. Was, E.A. Kenik, J. Nucl. Mater. 255 (1998) 44.
[7] K.D. Childs, B.A. Carlson, L.A. LaVanier, J.F. Moulder, D.F. Paul, W.F. Stickle, D.G. Watson, Handbook of Auger Electron Spectroscopy, third ed., Physical Electronics, Eden Praire, MN, 1995.
[8] N.K. Sheth, J.A. Manriquez, C.A. Freitas, J.M. Sanchez, M.T. Miglin, J.L. Nelson, in: Proceedings of the Sixth International Symposium on Environmental Degradation of Materials in Nuclear Power Systems Water Reactors, Ed. The Minerals, Metals and Materials Society, San Diego, CA, 1993.
[9] M.G. Burke, T.R. Mager, L.L. Nelson, in: Proceedings of the Sixth International Symposium on Environmental Degradation of Materials in Nuclear Power Systems Water Reactors, Ed. The Minerals, Metals and Materials Society, San Diego, CA, August, 1993.
[10] M. Gao, R.P. Wei, Scripta Metall. Mater. 32 (1995) 987.
[11] M. Gao, R.P. Wei, Scripta Metall. Mater. 37 (1997) 1843.
[12] X.J. Pang, D.J. Dwyer, M. Gao, P. Valerio, R.P. Wei, Scripta Metall. Mater. 31 (1994) 345.
[13] M. Chen, M.C. Chaturvedi, N.L. Richards, G. McMahon, Metall. Mater. Trans. 29A (1998) 1947.
[14] M. Hernández-Mayoral, G. De Diego, M. García-Mazarío, J. Nucl. Mater. 279 (2000) 189.
[15] J. Walmsley, P. Spellward, S. Fisher, A. Jenssen, in: Proceedings of the Seventh International Symposium on Environmental Degradation of Materials in Nuclear Power Systems Water Reactors, Ed. NACE, Breckenridge, CO, August 1995.
[16] C.C. Goodwin, R.G. Faulkner, S.B. Fisher, in: R.K. Nanstad, M.L. Hamilton, F.A. Garner, A.S. Kumar (Eds.), Proceedings of the 18th International Symposium on Effect of Radiation on Materials, ASTM STP 1325, American Society for Testing and Materials, p. 634.